The New High-Pressure Sodium Tetraborate HP-Na$_2$B$_4$O$_7$

Stephanie C. Neumair,[a] Gerhard Sohr,[a] Stefan Vanicek,[a] Klaus Wurst,[a] Reinhard Kaindl,[b] and Hubert Huppertz*[a]

Abstract. The new polymorph of sodium tetraborate HP-Na$_2$B$_4$O$_7$ was synthesized under high-pressure / high-temperature conditions of 6 GPa and 1000 °C in a multianvil apparatus with a Walker-type module. HP-Na$_2$B$_4$O$_7$ crystallizes with nine formula units per cell in the trigonal chiral space groups $P3_2$21 or $P3_1$21. The parameters are $a =$ 765.5(2), $c = 2142.3(4)$ pm, $V = 1.0872(3)$ nm^3, $R_1 = 0.0581$, and wR_2 = 0.0809 (all data). The crystal structure of HP-Na$_2$B$_4$O$_7$ is built up from interconnected "sechser" rings of alternating corner-sharing BO$_3$ and BO$_4$ groups.

Introduction

The ore borax (Na$_2$B$_4$O$_7$·10H$_2$O) has been known since the old ages, and still is one of the most important boron minerals mined today. Borax has many applications, e.g. it is used in glazes, as a component in detergents, or as welding flux,[1] but it is also the raw material for many boron chemicals. It crystallizes monoclinically in the space group C2/c exhibiting a fundamental building block of two six-membered rings formed by two BO$_3$ and two BO$_4$ units.[2–4] Next to other hydrated sodium tetraborates (e.g. kernite (Na$_2$B$_4$O$_7$·4H$_2$O)[1]), several anhydrous polymorphs of sodium tetraborate exist. All in all, five different sodium tetraborates have been reported (α-, β-, γ-, δ-, ε-Na$_2$B$_4$O$_7$[5–7]), but only for α-Na$_2$B$_4$O$_7$[5] and γ-Na$_2$B$_4$O$_7$[7] the detailed crystal structure is known. Both compounds are built up from corner-sharing BO$_3$ and BO$_4$ groups, yet α-Na$_2$B$_4$O$_7$[5] crystallizes in layers, whereas γ-Na$_2$B$_4$O$_7$[7] consists of a three-dimensional network structure. For β-, δ-, and ε-Na$_2$B$_4$O$_7$, literature research only reveals indexed powder diffraction patterns leading to possible space groups and lattice parameters.[6]

Due to the fact that anhydrous sodium borates are one of the main constituents of borosilicate glasses, the ternary system Na-B-O is well studied under ambient pressure. Various compositions and polymorphs thereof are known, e.g. β-Na$_2$B$_6$O$_{10}$,[8] α-/β-Na$_2$B$_8$O$_{13}$,[9,10] and Na$_3$B$_7$O$_{12}$.[11] When studying the structures of sodium borates, numerous fundamental building blocks (FBB) can be found forming complex B-O networks; yet most FBB can be divided into less complex borate building blocks. For instance, the compound β-Na$_2$B$_6$O$_{10}$ can be regarded as a double layer structure that is built up from a FBB consisting of three different groupings: a double ring pentaborate unit, a triborate ring, and a BO$_4$ tetrahedron.[8]

Interestingly, in this well studied system no high-pressure borates were known up to now. In this paper, we report about the new non-centrosymmetric high-pressure borate HP-Na$_2$B$_4$O$_7$. Next to the description of synthesis and structural details, the properties of the new sodium tetraborate are discussed.

Results and Discussion

Figure 1 depicts a view of the non-centrosymmetric crystal structure of HP-Na$_2$B$_4$O$_7$, which is built up from trigonal planar BO$_3$ units and slightly distorted BO$_4$ tetrahedra that are interconnected via corner-sharing. Three BO$_4$ tetrahedra and three BO$_3$ groups are connected alternatingly to form so-called "sechser"[12] rings ([B$_6$O$_{15}$]$^{12-}$ units, see Figure 2). Every "sechser" ring is part of six adjacent "sechser" rings, forming layers in the ab-plane. The layers are interconnected to a three-dimensional network structure, forming channels along the c-axis in which the sodium ions are situated. The interconnecting atoms are O4 (1× per "sechser" ring) and O6 (2× per "sechser" ring). Figure 3 depicts HP-Na$_2$B$_4$O$_7$ with a view along [100], showing a side view of six condensed layers of "sechser" rings, where the alternating connection scheme of one (O4) or two (O6) bridging oxygen atoms is viewed. Table 1, Table 2, and Table 3 list details of the data collection and evaluations as well as the positional parameters of the refinement.

"Sechser" rings with alternating BO$_4$ and BO$_3$ groups have been previously reported in borate chemistry for the compounds Li$_4$B$_7$O$_{12}$Cl[13] and H$_3$$REB_6O_{12}$ (RE = Sm–Lu).[14] In

* Univ.-Prof. Dr. H. Huppertz
  Fax: +43 (0)512 507 2934
  E-Mail: Hubert.Huppertz@uibk.ac.at
[a] Institut für Allgemeine, Anorganische und Theoretische Chemie
  Leopold-Franzens-Universität Innsbruck
  Innrain 52a
  6020 Innsbruck, Austria
[b] MATERIALS – Institut für Oberflächentechnologie und Photonik
  JOANNEUM RESEARCH Forschungsgesellschaft mbH
  Leobnerstraße 94
  8117 Niklasdorf, Austria
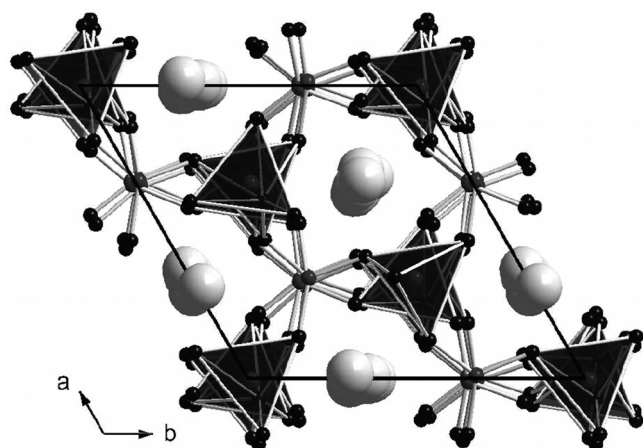 Supporting information for this article is available on the WWW under http://dx.doi.org/10.1002/zaac.201100363 or from the author.

WILEY
ONLINE LIBRARY

Figure 1. View of the crystal structure of HP-Na$_2$B$_4$O$_7$ along [001]. The structure is built up from "sechser" rings of alternating corner-sharing BO$_4$ and BO$_3$ units forming channels along the *c*-axis. Within these channels, the sodium ions are situated. Oxygen atoms: corners of polyhedra and small dark spheres, B: centre of polyhedra and small grey spheres, Na: large light spheres.
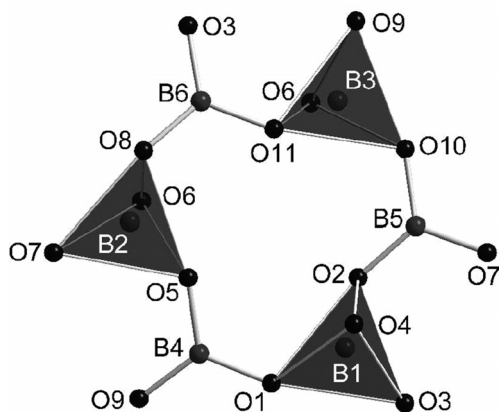

Figure 2. "Sechser" ring formed of three BO$_4$ units and three BO$_3$ units. The units are connected alternatingly via corner-sharing.
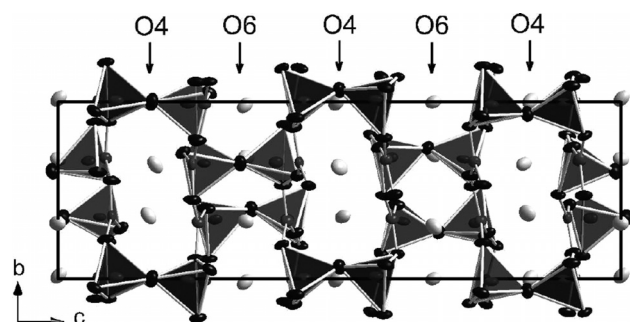

Figure 3. The crystal structure of HP-Na$_2$B$_4$O$_7$ with 90 % probability ellipsoids viewed along [100], showing a side view of six condensed layers of "sechser" rings. Oxygen atoms: corners of polyhedra and small dark spheres, B: center of polyhedra and small grey spheres, Na: large light spheres.

accordance with the pressure-coordination rule,[15] one would expect that higher pressures (usually > 7 GPa) lead to a structural transformation into denser phases that are exclusively

Table 1. Crystal data and structure refinement of HP-Na$_2$B$_4$O$_7$ (standard deviations in parentheses).

Empirical formula	Na$_2$B$_4$O$_7$
Molar mass /g·mol^{-1}	201.2
Crystal system	trigonal
Space group	$P3_221$
Powder diffractometer	STOE Stadi P
Radiation	Mo-$K_{\alpha 1}$ (λ = 70.93 pm)
Powder data	
a /pm	765.3(2)
c /pm	2141.4(5)
V /nm^3	1.0862(3)
Single crystal diffractometer	Enraf–Nonius Kappa CCD
Radiation	Mo-K_α (λ = 71.073 pm)
Single crystal data	
a /pm	765.5(2)
c /pm	2142.3(4)
V /nm^3	1.0872(3)
Formula units per cell	9
Calculated density /g·cm^{-3}	2.766
Crystal size /mm	0.11 × 0.08 × 0.07
Temperature /K	293(2)
Absorption coefficient /mm^{-1}	0.402
$F(000)$	882
θ range /°	1.9–35.0
Range in hkl	±12, ±12, –31/+34
Total no. of reflections	15178
Independent reflections	3214 (R_{int} = 0.0885)
Reflections with $I \geq 2\sigma(I)$	2744 (R_σ = 0.0579)
Data / parameters	3214 / 179
Absorption correction	multi-scan (Scalepack [52])
Goodness-of-fit on F_i^2	1.064
Final R indices [$I \geq 2\sigma(I)$]	R_1 = 0.0452
	wR_2 = 0.0779
R indices (all data)	R_1 = 0.0581
	wR_2 = 0.0809
Flack parameter	0.0(3)
Largest diff. peak and hole /e·Å^{-3}	0.34 / –0.70

built up from BO$_4$ tetrahedra. Astonishingly, up to now, further experiments with pressures up to 10 GPa did not yield in any other phases.

The B–O bond lengths of the BO$_4$ tetrahedra in HP-Na$_2$B$_4$O$_7$ vary between 143.2 and 150.2 pm with an average value of 147.6 pm. This mean value is consistent with the known average value of 147.6 pm for BO$_4$ tetrahedra.[16,17] Within the BO$_3$ unit of HP-Na$_2$B$_4$O$_7$, the B–O bond lengths vary from 135.9 to 138.1 pm with a mean value of 137.3 pm, which is slightly increased compared to the average value in the literature (137.0 pm).[18] These distances are similar to the ones found in Li$_4$B$_7$O$_{12}$Cl[13] and H$_3$*RE*B$_6$O$_{12}$ (*RE* = Sm–Lu).[14]

Figure 4 gives a view of the coordination spheres of the four crystallographically independent sodium ions according to the ECoN values (*E*ffective *Co*ordination *N*umbers[21–23]). Three of them (Na1, Na2, Na3) indicate a coordination number of eight (oxygen atoms), if values of ECoN smaller than 0.05 are neglected. The ion Na4 is surrounded by six oxygen atoms in a distorted octahedral way. In the eightfold coordination spheres around Na1, Na2, and Na3, the Na–O distances range from 226.5 to 297.5 pm. The mean distance of 251.0 pm is slightly lower than the average Na–O distance for eightfold coordi-

Table 3. Interatomic distances /pm in HP-$Na_2B_4O_7$ (space group $P3_221$), calculated with the single-crystal lattice parameters.

Na1–O11	231.7(2)	Na2–O3	232.7(2)	Na3–O2	2×	226.5(2)	
Na1–O7	234.6(2)	Na2–O10	237.4(2)	Na3–O6	2×	231.2(2)	
Na1–O5	235.1(2)	Na2–O1	238.6(2)	Na3–O11	2×	263.0(2)	
Na1–O3	242.6(2)	Na2–O6	240.9(2)	Na3–O5	2×	264.6(2)	
Na1–O4	249.6(2)	Na2–O9	247.4(2)			Ø = 246.3	
Na1–O9	254.0(2)	Na2–O7	264.1(2)				
Na1–O8	271.2(2)	Na2–O2	279.6(2)	Na4–O8	2×	225.0(2)	
Na1–O5	297.5(2)	Na2–O8	296.6(2)	Na4–O1	2×	251.4(2)	
	Ø = 252.0		Ø = 254.7	Na4–O10	2×	257.9(2)	
						Ø = 244.8	
B1–O4	143.2(2)	B2–O6	143.5(2)	B3–O6		145.3(2)	
B1–O1	148.0(2)	B2–O7	147.9(2)	B3–O9		147.8(2)	
B1–O3	149.2(2)	B2–O5	149.1(2)	B3–O11		147.8(2)	
B1–O2	150.2(2)	B2–O8	150.1(2)	B3–O10		148.8(2)	
	Ø = 147.7		Ø = 147.7			Ø = 147.4	
B4–O9	135.9(2)	B5–O10	137.7(2)	B6–O3		136.6(2)	
B4–O5	136.7(2)	B5–O2	137.5(2)	B6–O8		137.8(2)	
B4–O1	137.8(2)	B5–O7	137.5(2)	B6–O11		138.1(2)	
	Ø = 136.8		Ø = 137.5			Ø = 137.5	

nated sodium cations as it can be found e.g. in $NaVTeO_5$[22] for this coordination sphere (261.9 pm). The coordination distances of the sixfold coordinated sodium cation in HP-$Na_2B_4O_7$ vary from 225.0 to 257.9 pm with an average value of 244.8 pm, which tallies well with the mean value of 241.5 pm for $NaPO_3$.[23]

Due to the fact that HP-$Na_2B_4O_7$ is the third structurally characterized polymorph of sodium tetraborate (next to α-$Na_2B_4O_7$[5] and γ-$Na_2B_4O_7$[7]), a comparison between these three phases is compulsory. Table 4 lists all relevant details of the three different structures, whereas Figure 5 gives a comparative view of the crystal structures of α-$Na_2B_4O_7$[5] and γ-

Table 2. Atomic coordinates and equivalent isotropic displacement parameters U_{eq} /Å² of HP-$Na_2B_4O_7$ (space group $P3_221$). U_{eq} is defined as one third of the trace of the orthogonalized U_{ij} tensor (standard deviations in parentheses).

Atom	Wyckoff-Position	x	y	z	U_{eq}
Na1	6c	0.0054(2)	0.3560(2)	0.16086(3)	0.0140(2)
Na2	6c	0.7061(2)	0.6879(2)	0.33431(3)	0.0146(2)
Na3	3a	0	0.3236(2)	1/3	0.0121(2)
Na4	3b	0.3698(2)	0	1/6	0.0153(2)
O1	6c	0.2019(2)	0.1124(2)	0.24512(6)	0.0102(2)
O2	6c	0.8620(2)	0.0520(2)	0.26917(5)	0.0090(2)
O3	6c	0.9205(2)	0.7776(2)	0.24853(6)	0.0105(2)
O4	3b	0.9324(2)	0	1/6	0.0138(4)
O5	6c	0.2540(2)	0.4439(2)	0.23806(6)	0.0105(2)
O6	6c	0.2604(2)	0.6527(2)	0.32333(6)	0.0126(2)
O7	6c	0.5311(2)	0.7875(2)	0.24602(5)	0.0106(2)
O8	6c	0.1888(2)	0.7145(2)	0.22181(5)	0.0093(2)
O9	6c	0.5274(2)	0.3968(2)	0.26303(6)	0.0110(2)
O10	6c	0.5833(2)	0.1132(2)	0.26724(6)	0.0103(2)
O11	6c	0.8590(2)	0.4427(2)	0.24072(6)	0.0093(2)
B1	6c	0.9846(3)	0.9894(3)	0.2302(2)	0.0079(3)
B2	6c	0.3144(3)	0.6521(3)	0.2592(2)	0.0070(3)
B3	6c	0.6751(3)	0.3333(3)	0.2793(2)	0.0081(3)
B4	6c	0.3289(3)	0.3179(3)	0.24899(9)	0.0079(3)
B5	6c	0.6607(3)	0.9867(3)	0.26029(9)	0.0085(4)
B6	6c	0.9915(3)	0.6480(3)	0.23833(9)	0.0078(3)
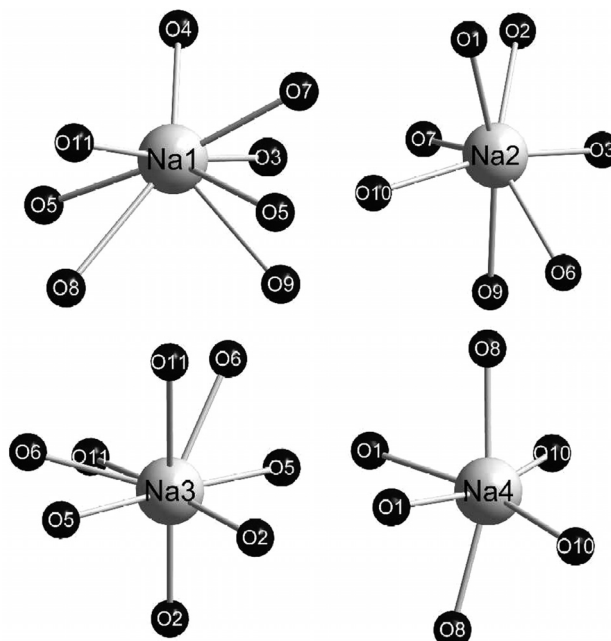
Figure 4. Coordination spheres of the four crystallographically independent Na⁺ ions in HP-$Na_2B_4O_7$.

$Na_2B_4O_7$ [7] and their main structural building units. All three phases are built up from corner-sharing BO_3 and BO_4 units. The compound α-$Na_2B_4O_7$ exhibits a non-bridging oxygen (O14), while in the other two phases all oxygen atoms bridge two boron atoms. In contrast to α-$Na_2B_4O_7$,[5] which exhibits a layer structure, HP-$Na_2B_4O_7$ and γ-$Na_2B_4O_7$[7] show three dimensional network structures. The average B–O bond lengths for the BO_3 and BO_4 units are very similar for α-$Na_2B_4O_7$ and γ-$Na_2B_4O_7$, while HP-$Na_2B_4O_7$ has slightly increased values. According to the fact that HP-$Na_2B_4O_7$ is synthesized under high-pressure / high-temperature conditions, this phase exhibits the highest density and the highest coordi-
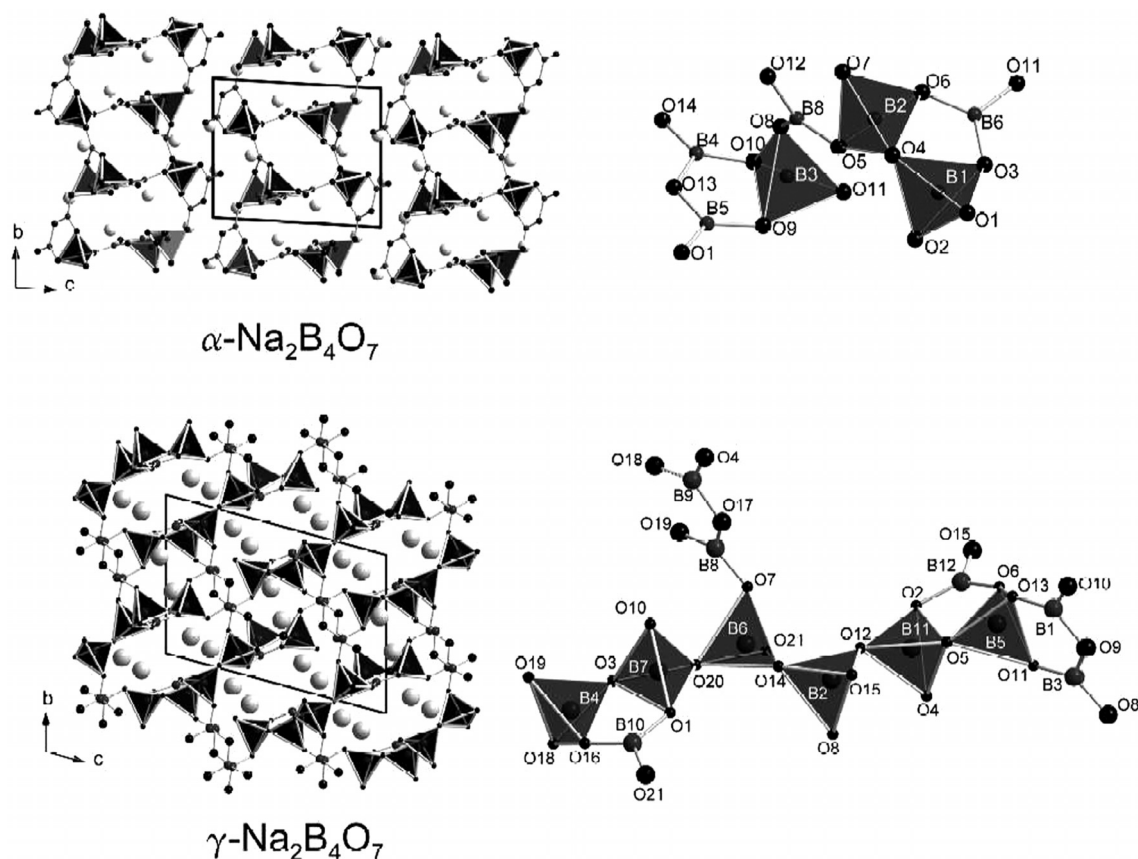
Figure 5. Comparison of the crystal structures of the two already known sodium tetraborates α-$Na_2B_4O_7$ (top, left) and γ-$Na_2B_4O_7$ (bottom, left) and their main structural building units (right).

nation numbers for three (Na1, Na2, Na3) of the four sodium atoms.

Table 4. Comparison of the different sodium tetraborate structures.

Compound	α-$Na_2B_4O_7$ [5]	γ-$Na_2B_4O_7$ [7]	HP-$Na_2B_4O_7$
Crystal system	triclinic	triclinic	trigonal
Space group	$P\bar{1}$	$P\bar{1}$	$P3_221$
a /pm	654.5(1)	670.5(1)	765.5(2)
b /pm	862.1(1)	960.1(2)	
c /pm	1048.6(1)	1327.2(3)	2142.3(4)
α /deg	93.28(1)	104.21(3)	
β /deg	94.87(1)	91.58(3)	
γ /deg	90.84(1)	106.40(3)	
Formula units per cell	4	6	9
Calculated density /g·cm⁻³	2.272	2.537	2.766
Coordination number at Na⁺	6, 7	5, 6, 7	6, 8
av. B–O distance, BO_3 unit	137.0 pm	137.0 pm	137.3 pm
av. B–O distance, BO_4 unit	147.4 pm	147.5 pm	147.6 pm

The MAPLE-values (*MA*delung *P*art of *L*attice *E*nergy)[19–21] were computed, in order to compare the results with the sum of the MAPLE-values received from Na_2O [24] and the high-pressure modification B_2O_3-II [25]. Therefore, the MAPLE-values from the binary oxides are summed up stoichiometrically, to calculate a hypothetical value for HP-$Na_2B_4O_7$. This resulted in a value of 46788 kJ·mol⁻¹ starting from the binary oxides (Na_2O (2912 kJ·mol⁻¹) + 2 × B_2O_3-II

(21938 kJ·mol⁻¹)[25]) to be compared with 47276 kJ·mol⁻¹ for HP-$Na_2B_4O_7$ (deviation: 1.0 %).

Furthermore, the bond valence sums for all atoms of HP-$Na_2B_4O_7$ were calculated, applying the bond length/bond-strength (ΣV)[26,27] and the CHARDI (*char*ge *di*stribution in solids, ΣQ) [28] concept (Table S1). The formal ionic charges of the atoms fit very well to the ones calculated with the CHARDI concept, but the values calculated with the bond length/bond-strength concept show rather large differences in the values for the sodium ion. Nevertheless, the formal ionic charges are consistent within the limits of the concepts.

In Figure 6 the FTIR transmission spectrum (recalculated from the ATR-absorbance) of HP-$Na_2B_4O_7$ in the range 600–1600 cm⁻¹ is displayed. The wavenumbers of 24 absorption bands are given in Table S2. Bands around 700 cm⁻¹ are typical for bending vibrations of BO_4 groups.[29–31] Between 800 cm⁻¹ and 1100 cm⁻¹, stretching vibrations of tetrahedrally coordinated boron atoms are expected.[29,32,33] The bands in the range of 1200–1450 cm⁻¹ were previously described as stretching vibrations of BO_3 groups.[34–37] Recently, the Author's group presented two studies about HP-KB_3O_5 and HP-LiB_3O_5,[38,39] which both are built up of three-dimensional networks of BO_4 tetrahedra and BO_3 groups with band assignments in the vibrational spectra based on ab initio calculations of the electronic structure. These calculations provided detailed

information about the contributions of BO$_4$ and BO$_3$ units to the spectral bands. In a very similar approach, *Sitarz* et al.[40] carried out model calculations and compared them with experimental spectra of silicates containing silicooxygen rings. They described stretching Si–O(Si) vibrations in the region 1100–1200 cm^{-1}, a stretching Si-O$^-$ vibration around 1000–800 cm^{-1}, from 800–600 cm^{-1} a band characteristic of silicooxygen rings, and below 600 cm^{-1} bending O–Si–O and (Si)O–Si–O(Si) modes. For six-membered rings, they found a "ring-band" at 610 cm^{-1}. The similarity of vibrational spectra containing tetrahedral XO_4 groups (X = Si, P, S) was shown for example by *Nasdala* et al.[41] in 2004. For HP-Na$_2$B$_4$O$_7$, calculations are not available up to now but assignments by analogy to the above mentioned borates and silicates should be applicable to HP-Na$_2$B$_4$O$_7$ as well, of course with uncertainties due to the lower mass of boron compared to silicon and the presence of alternating BO$_4$ and BO$_3$ units in the rings. In the spectrum of HP-Na$_2$B$_4$O$_7$, three strong absorption bands at 634, 671, and 784 cm^{-1} are observed. This agrees nicely with the results from the X-ray diffraction study because the "sechser rings" in this structure are built up of alternating BO$_4$ and BO$_3$ units. This most probably results in a splitting of the one "ring band" which originates from rings exclusively built up of tetrahedrally coordinated units, into two or more bands with slightly different wavenumbers in the "mixed" rings. The shift to higher wavenumbers of the split "ring bands" is consistent with the lower mass and bond lengths of B–O in contrast to Si–O units.
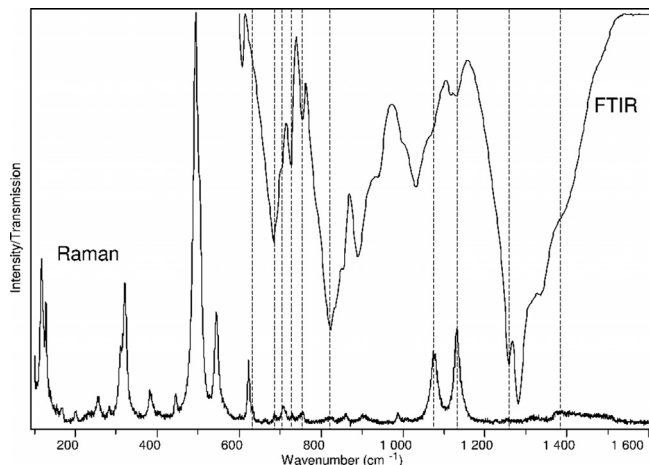

Figure 6. FTIR transmission and Raman spectrum of a HP-Na$_2$B$_4$O$_7$ single crystal in the range 100–1600 cm^{-1}. The FTIR transmission was recalculated from the ATR-absorbance. The dotted lines indicate approximately the same positions of Raman and FTIR bands.

In the higher wavenumber range 1600–4000 cm^{-1} (not displayed) absorption bands caused by organic contaminations (2860–2960 cm^{-1}, probably nail polish) are observed, but also bands around 1635–1800 and 3200–3600 cm^{-1}. These bands are usually assigned to bending and stretching vibrations of H$_2$O or OH molecules, suggesting possibly small amounts of hydrous species bonded in the structure.

The vertical broken lines in Figure 6 mark vibrational bands which occur in both the FTIR absorption and the Raman spectrum. In structures with a centre of inversion, IR- and Raman-active modes at the same wavenumber are forbidden by the selection rules.[42] The occurrence of modes in both IR and Raman spectra support the finding from X-ray diffraction that HP-Na$_2$B$_4$O$_7$ crystallizes in a non-centrosymmetric structure.

The Raman spectrum and the corresponding wavenumbers of bands of a HP-Na$_2$B$_4$O$_7$ single crystal are displayed in Figure 6 and Table S3. In total, 35 bands in the range of 100–1600 cm^{-1} could be detected. Above 1600 cm^{-1}, no bands were observed which is consistent with only small amounts of H$_2$O or OH molecules in the structure.

The most intense band in the spectrum at 494 cm^{-1} is flanked by several bands of medium intensity at 505, 545, and 623 cm^{-1}. Above 1000 cm^{-1}, two medium intensity bands at 1076 and 1132 cm^{-1} are followed by a few weak bands at 1255, 1317, 1393, and 1476 cm^{-1}. Below 500 cm^{-1}, two medium intensity double bands at 321, 310, 128, and 117 cm^{-1} are detected. Generally, bands below 800 cm^{-1} in borates are assigned to bending vibrations of the BO$_4$ tetrahedra, vibrations related to cation–oxygen bonds, and complex lattice vibrations (e.g.[38,39]).

In the range from 800–1100 cm^{-1}, stretching vibrations of BO$_4$ tetrahedra are expected. Above 1100 cm^{-1}, Raman modes were described for edge-sharing BO$_4$ tetrahedra and BO$_3$ groups.[38,43] In contrast to the mentioned compounds, they are rather weak and broad, suggesting energy levels of the stretching vibrations of the ([B$_6$O$_{15}$]$^{12-}$ units in the "sechser" rings.

Conclusions

The new non-centrosymmetric high-pressure polymorph of sodium tetraborate HP-Na$_2$B$_4$O$_7$ was synthesized utilizing a multianvil press with a modified Walker-type module. HP-Na$_2$B$_4$O$_7$ is built up from BO$_3$ and BO$_4$ units that are connected alternatingly forming layers of "sechser" rings. The layers are interconnected to a three-dimensional network structure, forming channels along the c-axis in which the sodium ions are located.

Experimental Section

Synthesis

The new polymorph of sodium tetraborate HP-Na$_2$B$_4$O$_7$ was synthesized under high-pressure / high-temperature conditions of 6 GPa and 1000 °C. Therefore, a stoichiometric mixture of Na$_2$CO$_3$ (ChemPur, Karsruhe, Germany, 99.9 %) and H$_3$BO$_3$ (Merck KGaA, Darmstadt, Germany, 99.5 %) was ground together and heated at 850 °C for 12 h to expel the volatile components (H$_2$O, CO$_2$). To gain HP-Na$_2$B$_4$O$_7$, the amorphous reaction product was compressed and heated in a multianvil press. For this purpose, the reaction product was reground, filled into a boron nitride crucible (Henze BNP GmbH, HeBoSint® S100, Kempten, Germany), and placed inside an 18/11-octahedral pressure medium. The assembly was compressed and heated in a multianvil device based on a Walker-type module and a 1000 t press (both devices from the company Voggenreiter, Mainleus, Germany). A detailed description of the assembly preparation can be found in refs.[44–48]. For the high-pressure / high-temperature experiment, the

sample was compressed to 6 GPa in 3 h, then heated to 1000 °C in 10 minutes and kept there for 10 minutes. Afterwards, the sample was cooled down to 400 °C in 40 minutes and naturally cooled down to room temperature by switching off the heating. After a decompression period of 8.5 h, the sample was carefully separated from the surrounding boron nitride crucible. The new compound HP-$Na_2B_4O_7$ was gained in the form of colorless, air-resistant crystals. Further experiments up to 10 GPa yielded in the same compound.

Crystal Structure Analysis

The powder X-ray diffraction pattern of HP-$Na_2B_4O_7$ was measured in transmission geometry from flat samples of the reaction product by using a Stoe Stadi P powder diffractometer with Ge-111-monochromatized Mo-$K_{\alpha 1}$ radiation (λ = 70.93 pm). Figure S1 depicts the measured diffraction pattern as well as the theoretical pattern simulated from single-crystal data, proving the purity of the obtained HP-$Na_2B_4O_7$. The reflections of the sodium tetraborate were indexed with TREOR [49–51] on the basis of a trigonal unit cell (Table 1). This confirmed the lattice parameters, received from the single-crystal X-ray diffraction study.

For the single-crystal X-ray diffraction data collection, small irregularly shaped single crystals of the sodium borate HP-$Na_2B_4O_7$ were isolated by mechanical fragmentation. The single crystal intensity data of HP-$Na_2B_4O_7$ were obtained at room temperature on a Nonius Kappa-CCD diffractometer with graphite monochromatized Mo-K_a radiation (λ = 71.073 pm). A semi-empirical absorption correction was applied to the intensity data (Scalepack [52]). Based on the systematically absent reflections, the possible space groups $P3_1$, $P3_2$, $P3_121$, $P3_221$, $P3_112$, $P3_212$, $P6_2$, $P6_4$, $P6_222$, and $P6_422$ were derived. As no solution could be obtained by Direct Methods with the SHELX-97 software suite,[53,54] the structure was solved with Direct Methods in SIR2004[55] in the space group $P3_221$. The crystal was merohedrally twinned and the parameter refinement (full-matrix least-squares against F^2) were carried out with the twin matrix 100 010 00$\bar{1}$ improving the R_1-value from 0.095 (without matrix) to 0.045. The twin ratio converged to a value of around 6:1. Interestingly, the twin element is a mirror plane perpendicular to the reciprocal c^*-axis and this implies that the minor part of the twin crystallizes in the enantiomorphic chiral space group $P3_121$. As no additional symmetry could be found, the structure is non-centrosymmetric; the Flack parameter converged to a value of 0.0(3). All atoms were refined with anisotropic displacement parameters. Final difference Fourier syntheses did not reveal any significant peaks in the refinements. Details of the data collection and structure elucidation are listed in Table 1. Table 2 and Table 3 list the positional parameters of the refinements as well as the interatomic distances. Additional details of the crystal structure investigations may be obtained from the Fachinformationszentrum Karlsruhe (crysdata@fiz-karlsruhe.de, http://www.fizinformationsdienste.de/en/DB/icsd/ depotanforderung.html), 76344 Eggenstein-Leopoldshafen, Germany on quoting the Registry No. CSD-423429.

IR Spectroscopy

FTIR-ATR (**A**ttenuated **T**otal **R**eflection) spectra of single crystals were recorded with a Bruker Vertex 70 FT-IR spectrometer (spectral resolution 4 cm^{-1}), attached to a Hyperion 3000 microscope in a spectral range from 600–4000 cm^{-1}. A frustum-shaped germanium ATR-crystal with a tip diameter of 100 μm was pressed on the surface of the borate crystal with a power of 5 N which crushed it into pieces of μm-size. 64 scans for the sample and the background were acquired.

Beside spectra correction for atmospheric influences, an enhanced ATR-correction [56], using the OPUS 6.5 software, was performed. A mean refraction index of the sample of 1.6 was assumed for the ATR-correction. Background correction and peak fitting followed via polynomial and folded Gaussian-Lorentzian functions.

Raman Spectroscopy

Confocal Raman spectra of single crystals were obtained with a HORIBA JOBIN YVON LabRam-HR 800 Raman micro-spectrometer. The sample was excited by the 532 nm emission line of a 30 mW Nd-YAG-laser under an OLYMPUS 100× objective (N.A. = 0.9). The size and power of the laser spot on the surface were approximately 1 μm and 0.5 mW, respectively. The scattered light was dispersed by a grating with 1800 lines/mm and collected by a 1024× 256 open electrode CCD detector. The spectral resolution, determined by measuring the Rayleigh line, was about 1.4 cm^{-1}. Third order polynomial and convoluted Gauss-Lorentz functions were applied for background correction and band fitting. The wavenumber accuracy of about 0.5 cm^{-1} was achieved by adjusting the zero-order position of the grating and regularly checked by a neon spectral calibration lamp.

References

[1] A. F. Holleman, E. Wiberg, N. Wiberg in *Lehrbuch der Anorganischen Chemie*, Walter de Gruyter, Berlin, New York, **2007**, vol. 102, pp. 1043–1047.

[2] N. Morimoto, *Mineral. J.* **1956**, *2*, 1–18.

[3] H. A. Levy, G. C. Lisensky, *Acta Crystallogr., Sect. B* **1978**, *34*, 3502–3510.

[4] G. J. Gainsford, T. Kemmitt, C. Higham, *Acta Crystallogr., Sect. E* **2008**, *64*, i24–i25.

[5] J. Krogh-Moe, *Acta Crystallogr., Sect. B* **1974**, *30*, 578–582.

[6] H. Li, J. Liang, *J. Am. Ceram. Soc.* **1995**, *78*, 470–478.

[7] A. S. Kanishcheva, A. V. Egorysheva, Yu. E. Gorbunova, Yu. F. Kargin, Yu. N. Mikhailov, V. M. Skorikov, *Z. Neorg. Khim.* **2004**, *49*, 1006–1011.

[8] J. Krogh-Moe, *Acta Cystallogr. Sect. B* **1972**, *28*, 1571–1576.

[9] R. S. Bubnova, Ju. F. Shepelev, N. A. Sennova, S. K. Filatov, *Z. Kristallogr.* **2002**, *217*, 444–450.

[10] N. Penin, M. Touboul, G. Nowogrocki, *J. Solid State Chem.* **2002**, *168*, 316–321.

[11] N. Penin, M. Touboul, G. Nowogrocki, *J. Alloys Compd.* **2004**, *363*, 104–111.

[12] The term "sechser" ring was initially coined by F. Liebau in his book Structural Chemistry of Silicates (Springer, Berlin, **1985**). It is derived from the german word "sechs", which means six. However, a "sechser" ring is not a six membered ring, but a ring with six tetrahedral centers (B). Similar terms exist for rings made up of two or three tetrahedral centers, namely "zweier" and "dreier" rings.

[13] W. Jeitschko, T. A. Bither, P. E. Bierstedt, *Acta Crystallogr., Sect. B* **1977**, *33*, 2767–2775.

[14] L. Li, P. Lu, Y. Wang, X. Jin, G. Li, Y. Wang, L. You, J. Lin, *Chem. Mater.* **2002**, *14*, 4963–4968.

[15] A. Neuhaus, *Chimia* **1964**, *18*, 93–103.

[16] E. Zobetz, *Z. Kristallogr.* **1990**, *191*, 45–57.

[17] F. C. Hawthorne, P. C. Burns, J. D. Grice in *Boron: Mineralogy, Petrology and Geochemistry* (Ed.: E. S. Grew), Mineralogical Society of America, Washington, **1996**, p. 44.

[18] E. Zobetz, *Z. Kristallogr.* **1982**, *160*, 81–92.

[19] P. Rozier, L. Vendier, J. Galy, *Acta Crystallogr., Sect. C* **2002**, *58*, i111–i113.

[20] K. H. Jost, *Acta Crystallogr.* **1963**, *16*, 428.

[21] R. Hoppe, *Angew. Chem.* **1966**, 78, 52–63; *Angew. Chem. Int. Ed. Engl.* **1966**, *5*, 95–106.

[22] R. Hoppe, *Angew. Chem.* **1970**, 82, 7–16; *Angew. Chem. Int. Ed. Engl.* **1970**, *9*, 25–34.

[23] R. Hübenthal, *Maple*, Program for the Calculation of Maple Values (Vers. 4) University of Giessen, Giessen, Germany, **1993**.

[24] E. Zintl, A. Harder, B. Dauth, *Z. Elektrochem.* **1934**, *40*, 588–593.

[25] C. T. Prewitt, R. D. Shannon, *Acta Crystallogr., Sect. B* **1968**, *24*, 869–874.

[26] I. D. Brown, D. Altermatt, *Acta Crystallogr., Sect. B* **1985**, *41*, 244–247.

[27] N. E. Brese, M. O'Keeffe, *Acta Crystallogr., Sect. B* **1991**, *47*, 192–197.

[28] R. Hoppe, S. Voigt, H. Glaum, J. Kissel, H. P. Müller, K. J. Bernet, *J. Less-Common Met.* **1989**, *156*, 105–122.

[29] J. P. Laperches, P. Tarte, *Spectrochim. Acta* **1966**, *22*, 1201–1210.

[30] G. Heymann, K. Beyer, H. Huppertz, *Z. Naturforsch.* **2004**, *59B*, 1200–1208.

[31] C. E. Weir, R. A. Schroeder, *J. Res. Nat. Bur. Stands.* **1964**, *68A*, 465–487.

[32] M. Ren, J. H. Lin, Y. Dong, L. Q. Yang, M. Z. Su, L. P. You, *Chem. Mater.* **1999**, *11*, 1576–1580.

[33] G. Blasse, G. P. M. van den Heuvel, *Phys. Status Solidi* **1973**, *19*, 111–117.

[34] S. D. Ross, *Spectrochim. Acta* **1972**, *28A*, 1555–1561.

[35] W. C. Steele, J. C. Decius, *J. Chem. Phys.* **1956**, *25*, 1184–1188.

[36] R. Böhlhoff, H. U. Bambauer, W. Hoffmann, *Z. Kristallogr.* **1971**, *133*, 386–395.

[37] K. Machida, H. Hata, K. Okuno, G. Adachi, J. Shiokawa, *J. Inorg. Nucl. Chem.* **1979**, *41*, 1425–1430.

[38] S. C. Neumair, S. Vanicek, R. Kaindl, D. M. Többens, C. Marti-neau, F. Taulelle, J. Senker, H. Huppertz, *Eur. J. Inorg. Chem.* **2011**, 4147–4152.

[39] S. C. Neumair, S. Vanicek, R. Kaindl, D. M. Többens, K. Wurst, H. Huppertz, *J. Solid State Chem.* **2011**, *184*, 2490–2497.

[40] M. Sitarz, M. Handke, W. Mozgawa, *Spectrochim. Acta* **1999**, *55A*, 2831–2837.

[41] L. Nasdala, D. Smith, R. Kaindl, M. Ziemann, *Spectroscopic Methods in Mineralogy* (Eds.: A. Beran, E. Libowitzky) Eötvös University Press, Budapest, **2004**, pp. 281–343.

[42] D. C. Harris, M. D. Bertolucci, *Symmetry and Spectroscopy: an Introduction to Vibrational and Electronic Spectroscopy*, Oxford University Press, New York, **1989**.

[43] S. C. Neumair, R. Kaindl, H. Huppertz, *J. Solid State Chem.* **2011**, *184*, DOI:10.1016/j.jssc.2011.10.028.

[44] D. Walker, M. A. Carpenter, C. M. Hitch, *Am. Mineral.* **1990**, *75*, 1020–1028.

[45] D. Walker, *Am. Mineral.* **1991**, *76*, 1092–1100.

[46] H. Huppertz, *Z. Kristallogr.* **2004**, *219*, 330–338.

[47] D. C. Rubie, *Phase Transitions* **1999**, *68*, 431–451.

[48] N. Kawai, S. Endo, *Rev. Sci. Instrum.* **1970**, *41*, 1178–1181.

[49] *Treor90*, P.-E. Werner, University of Stockholm, **1990**.

[50] P.-E. Werner, *Z. Kristallogr. Kristallgeom. Kristallphys. Kristallchem.* **1964**, *120*, 375–387.

[51] P.-E. Werner, L. Errikson, M. Westdahl, *J. Appl. Crystallogr.* **1985**, *18*, 367–370.

[52] Z. Otwinowski, W. Minor, *Methods Enzymol.* **1997**, *276*, 307–326.

[53] G. M. Sheldrick, *SHELXS-97* and *SHELXL-97*, Program suite for the solution and refinement of crystal structures, University of Göttingen, Göttingen, Germany, **1997**.

[54] G. M. Sheldrick, *Acta Crystallogr., Sect. A* **2008**, *64*, 112–122.

[55] M. C. Burla, R. Caliandro, M. Camalli, B. Carrozzini, G. L. Cascarano, L. De Caro, C. Giacovazzo, G. Polidori, R. Spagna, *J. Appl. Crystallogr.* **2005**, *38*, 381–388.

[56] F. M. J. Mirabella, Principles, Theory, and Practice of Internal Reflection Spectroscopy. In: *Internal Reflection Spectroscopy, Theory and Applications. Practical Spectroscopy Series* (Ed.: F. M. J. Mirabella), Marcel Dekker Inc., New York, **1993**, vol. 15, pp 17–53.